Electrical Properties of an Individual Chicken Infectious Laryngotracheitis Virus

Application of an atomic force microscopy-based technique.

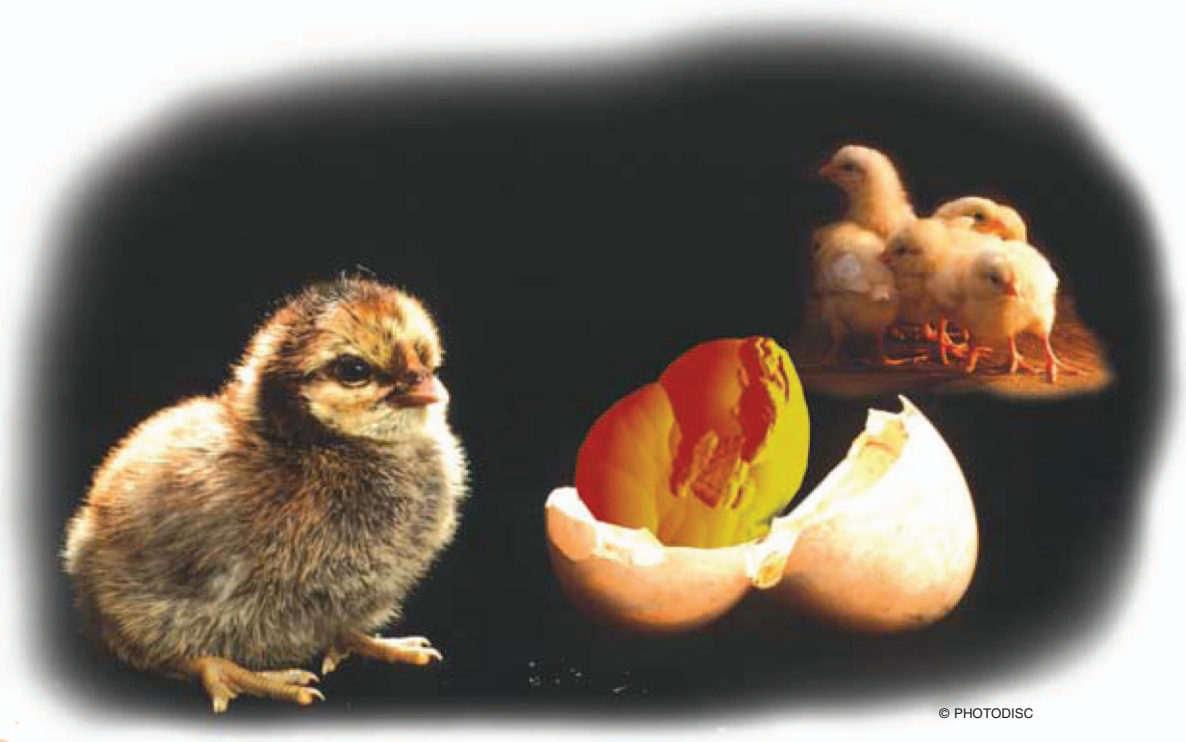

© PHOTODISC

OVER THE PAST FEW YEARS, VIRUS detection techniques have become increasingly important because of the frequent occurrence of new pathogenic virus strains. At present, there are two well-established diagnostic techniques for viruses: immunoassay and DNA-/RNA-based methods [1]. Immunoassay, considered the gold standard, uses either direct immunofluorescent assay or membrane enzyme-linked immunosorbent assay to first isolate the virus and then characterize it using serological or other molecular biological tools. Typical drawbacks for immunoassay include poor specificity and low sensitivity. By comparison, DNA-/RNA-based methods such as reverse transcription-polymerase chain reaction assays are much more specific and sensitive. These methods, however, are typically very time consuming since the protocol requires a series of DNA/RNA isolation, concentration, and gel electrophoresis.

STEVE TUNG, MICHAEL B. SCHULTE, ZHUXIN DONG, JIN-WOO KIM, UCHE WEJINYA, HYUNG-MO MOON, AND BYUNG-WHI KONG

Digital Object Identifier 10.1109/MNANO.2010.938019

1932-4510/10/$26.00©2010IEEE

An alternative approach in virus detection can be direct measurement of the material properties of individual virus particles. Previously, atomic force microscopy (AFM), as shown in Figure 1, has been demonstrated to be an excellent characterization tool not only in measuring the topography of nanoscale biomolecules such as DNA at high resolutions but also in determining the mechanical properties of individual avian influenza virus particles through nanoindentation [2]. This article describes the application of a similar AFM-based technique to determine the electrical properties of individual infectious laryngotracheitis virus (ILTV) particles. Specifically, the ILTV's electrical properties were measured in the form of ac impedance spectrum, as the virus particle was sandwiched between a conductive AFM tip and a conductive indium tin oxide (ITO) substrate. ILTV is one of the most contagious viruses that can cause severe health problems in chicken flocks. For states like Arkansas, ILTV outbreaks can lead to significant financial losses in the poultry industry. It is hypothesized that the viral electrical properties can be used to specifically identify ILTV through impedance spectroscopy. Confirmation of the hypothesis will be a breakthrough in the detection, classification, and isolation of ILTV.

A high stiffness coefficient will lead to potential sample damage, while a low stiffness coefficient will result in poor electrical contact between the tip and the virus.

MATERIALS AND METHODS

VIRUS SAMPLE PREPERATION

ILTV is a member of a large Herpesviridae family. For the present study, the United States Department of Agriculture (USDA) reference strain was purchased from the National Veterinary Services Laboratory (NVSL). The stock ILTV titer, which is defined as plaque-forming unit per milliliter (pfu/mL), was 10^5 pfu/mL. Generally, one pfu titer consists of 10^3–10^7 individual virus particles (termed virion). Thus, the ILTV stock is estimated to consist of approximately 10^8–10^{12} virion/mL. For both inactivation and fixation of ILTV, 200-μL ILTV stock was mixed with paraformaldehyde to become a 4% concentration. To verify virus inactivation, the ILTV suspension was used to infect cultured cells, and the plaque formation was monitored for virus propagation. The virus sample used in the present study was confirmed to be inactive when no live ILTV propagation was observed.

The preparation procedure of the AFM samples is as follows. First, 10× dilutions of the inactivated stock virus samples were prepared using deionized water. Next, each AFM sample was prepared by depositing 100 μL of the virus suspension on an ITO substrate. The samples were then allowed to air dry in optimal environmental conditions in a biological fume hood.

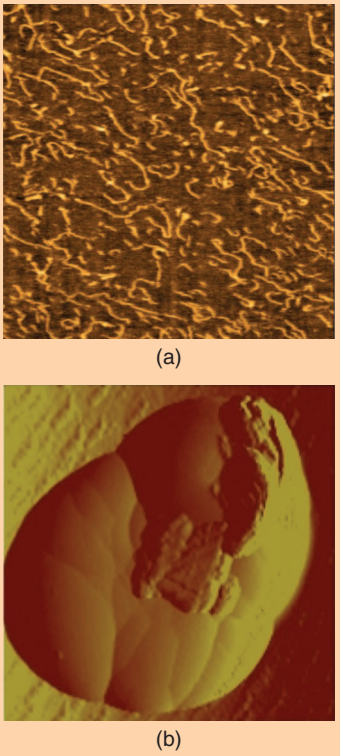

FIGURE 1 AFM-based analysis of biomolecules. (a) Topography of a 3,000-bp double-stranded DNA. (b) An avian influenza virus particle with an indented top surface created by an AFM tip.

EXPERIMENTAL SETUP

An Agilent 5500 AFM was used for electrical characterization work. The AFM software provides a current sensing AFM (CSAFM) function under contact mode. In this mode, an external impedance analyzer can be connected to the AFM for signal processing. CSAFM requires a special 10° nose cone containing a preamplifier. A bias voltage is applied to keep the AFM probe tip as a virtual ground. For the study, a current-sensing conductive AFM probe on a 10-μm scanner was put into the AFM. The probe consists of a Cr-/Pt-plated silicon tip with < 25 nm radius and a spring constant of $0.2 + 50\%$ N/m. The resonant frequency is 13 kHz.

To carry out ac impedance measurements that require a closed circuit for the frequency sweep, hookup wires were attached to the AFM nose cone's spring that holds the AFM probe and also to the virus sample's conductive surface. This surface consists of a 1,500-Å conductive ITO layer that serves as a ground plane for electrical characterization.

IMPEDANCE MEASUREMENT

Electrical impedance is a term that describes the opposition of a material/structure to a sinusoidal alternating current. In the present study, a small ac signal is applied to individual virus particles, and the corresponding absolute impedance Z and phase angle θ of the system are recorded. Based on this information, the electrical resistance R and reactance X of the virus particle are determined by using the following equations:

$$R = Z\cos(\theta),$$
$$X = Z\sin(\theta).$$

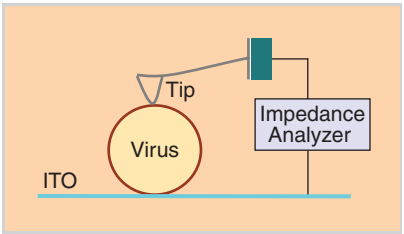

FIGURE 2 Schematic of the impedance measurement.

> Atomic force microscopy has been demonstrated to be an excellent characterization tool not only in measuring the topography of nanoscale biomolecules but also in determining the mechanical properties of individual avian influenza virus particles.

Figure 2 shows a schematic of the virus–AFM–impedance analyzer experimental setup. In this setup, the particle is sandwiched between the ITO substrate and the conductive AFM probe tip. The impedance analyzer (HP 4192A) sends a small sinusoidal signal to the virus through the conductive tip, records the current response, and computes the impedance value. Selecting an AFM tip with the proper stiffness coefficient is critical to this electrical characterization process. A high stiffness coefficient will lead to potential sample damage [see Figure 1(b)], while a low stiffness coefficient will result in poor electrical contact between the tip and the virus.

Impedance data were measured in the frequency range of 10 kHz to 1 MHz at increments of 10 kHz. The peak-to-peak voltage is 1 VAC. PC-based LabView was used to control the impedance analyzer through a general-purpose interface bus (GPIB). A standard LabView program was developed to read the GPIB card from the impedance analyzer.

EQUIVALENT CIRCUIT AND ZVIEW

After the impedance data were recorded, the information was converted into the corresponding resistance and reactance data and plotted using the PC program ZView. The ZView curve fits the data with equivalent circuit models of the measurement system, as shown in Figure 3, and calculates the model's components to determine the virus capacitance values [3]. In Figure 3, the constant phase element (CPE1) is a frequency-dependent component that represents the hardware elements of the AFM system, including the AFM tip and leakage current.

As described in [3], ZView is a strong program for calculating the components of an equivalent circuit. It consists of preprogrammed equivalent circuits as well as an option to create new circuit models. ZView also allows for impedance data to be inserted as a text file in resistance and capacitance versus frequency form into an existing plot. There are curve-fitting options to allow an equivalent circuit to be fitted to the plot. The circuit components can be made constant or variable, and the variable elements are then calculated.

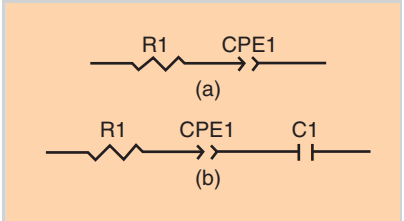

FIGURE 3 Equivalent circuit models. (a) Without and (b) with virus. R1, instrument resistance; CPE1, constant phase element of the instrument and its surroundings; C1, capacitance of the virus.

VIRUS DIELECTRIC CONSTANT MEASUREMENT

To determine the electrical properties of the virus, the resistance of the instrument and CPE must be determined. Impedance measurements were carried out using a similar experimental setup (Figure 2), except with the AFM tip touching the ITO substrate, thus closing the circuit. The measured impedance data were fitted with the equivalent circuit model shown in Figure 3(a). The result was used to calculate R1 and CPE1 of the equivalent circuit.

An identical procedure was employed to characterize the virus samples. Using the experimental setup shown in Figure 2, impedance measurements were made. The data were then fitted with the equivalent circuit model shown in Figure 3(b). Since the values of R1 and CPE1 have already been determined, the curve-fitting result yields the capacitance C1 of the virus particle.

In addition to virus particles, the impedance of polystyrene nanobeads was also characterized to verify the validity of the AFM method. For this study, nanobeads of similar size (diameter $\sim$ 200 nm) as the ILTV were chosen as the reference sample. Based on previous studies, the dielectric constant of polystyrene beads is approximately 2.6 [4]. Knowing this value as well as the capacitance values of the nanobead and virus, the dielectric constant of the virus can be approximated by the following equation [5]:

$$\varepsilon_v = \frac{C_v}{C_b}\varepsilon_b.$$

Here, ε_v is the dielectric constant of the virus, ε_b is the dielectric constant of the nanobead, C_v is the capacitance of the virus, and C_b is the capacitance of the nanobead.

EXPERIMENTAL RESULTS

AFM topographical images of the ITO substrate, polystyrene nanobeads, and virus samples are shown in Figure 4. As expected, the ITO surface is determined to be extremely smooth when compared with the surfaces immobilized with nanobeads and viruses. This is an important criteria for achieving high-resolution

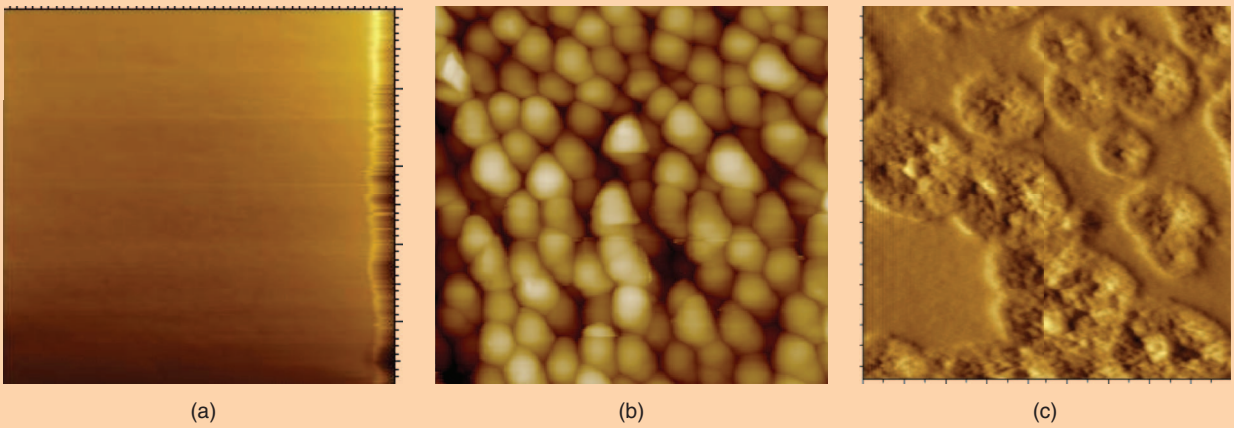

FIGURE 4 Topographical images measured by Agilent AFM. (a) ITO substrate, (b) polystyrene nanobeads, and (c) ILTV.

scans of nanoscale samples. The nanobead image displays clusters of well-defined, round-shaped structures whose average height corresponds very well to the vendor-supplied information of 200 nm. In the image, the virus particles appear as distinct disklike structures. The average diameter of the disk structures is approximately 200 nm, which agrees well with the established structural information of ILTV. Since the virus particles are inactivated, the height of the disks is only in the range of tens of nanometers, indicating that the virus structures have collapsed. Similar results have previously been observed in the AFM scanning of avian influenza viruses [2].

Figure 5 demonstrates the absolute impedance spectra of the ITO substrate, nanobead, virus, and buffer control, as measured by the impedance analyzer. These results are averaged results based on multiple experimental runs, and the degree of repeatability is high. The control, ITO, is shown to possess the lowest impedance value within the frequency range examined. The impedance values of the nanobead, buffer, and virus are all distinctively higher, with the largest difference occurring in the low-frequency range of the spectrum. The average difference in absolute impedance between the virus and ITO substrate is more than 30%. It can be observed that the absolute impedance of the virus is also different from that of the polystyrene nanobead.

The impedance analyzer (HP 4192A) sends a small sinusoidal signal to the virus through the conductive tip, records the current response, and computes the impedance value.

The absolute impedance data were further processed to generate the corresponding resistance and reactance information, which was then inserted into ZView for curve fitting based on equivalent circuit models. Figure 5 demonstrates the average capacitance values of the nanobead, buffer control, and virus

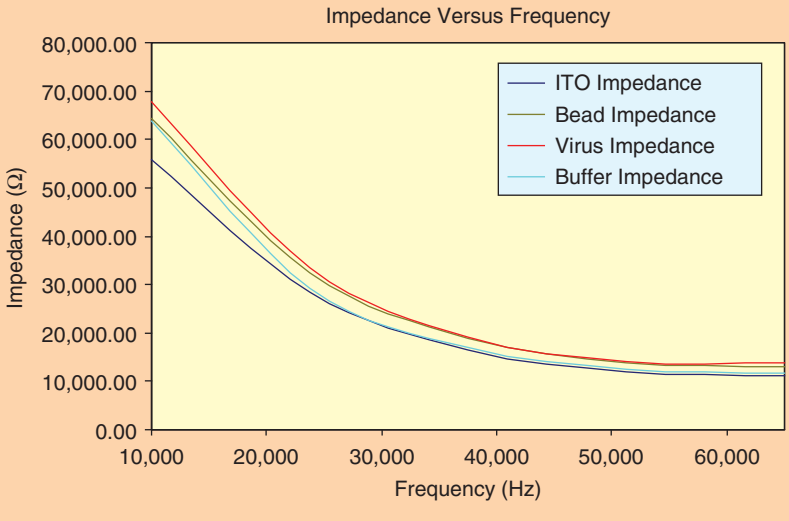

FIGURE 5 Absolute impedance spectra of ITO substrate, nanobead, virus, and buffer control.

Electrical impedance is a term that describes the opposition of a material/structure to a sinusoidal alternating current.

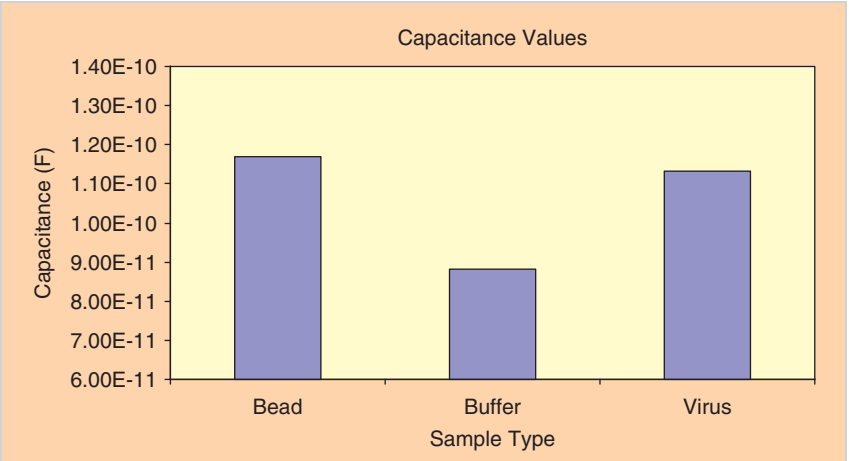

FIGURE 6 Capacitance of nanobead, buffer control, and virus.

particle. It is evident that the capacitance values of the nanobead and virus particle are significantly different from that of the buffer control. The average capacitance of the nanobead is about 6.5 nF, while that of the virus is about 6 nF.

Based on the capacitance results, the dielectric constant of the ILTV was calculated using the previously described equation. The value was determined to be approximately 2.4. This is slightly lower than that of the polystyrene nanobead.

CONCLUSIONS

This article investigates the electrical properties of individual ILTV particles using AFM and compares these properties with that of various control materials to determine the validity of identifying ILTV based on their unique material properties. The result indicates that the absolute impedance of a single ILTV particle in the frequency range of 10–65 kHz is about 30% higher than that of the bare conductive substrate on which the viral impedance value is measured. By curve fitting the experimental data with an equivalent circuit model of the measurement system, the average capacitance of the virus particle is determined to be approximately 6 nF. By comparing this capacitance value with that of a polystyrene nanobead of similar dimensions, the dielectric constant of the virus particle is determined to be approximately 2.4.

The current result indicates that it is indeed possible to identify ILTV based on its electrical properties when compared with abiological materials of similar nanoscale dimensions. However, additional studies will be required to determine whether it is possible to identify ILTV among biological materials such as other virus strains of similar dimensions. With known differences between ILTV and control properties, an electrical detection scheme of ILTV can be developed to provide fast, on-site diagnostics. Such a system will equip poultry farmers with the ability to exercise quick response to ILTV outbreaks and prevent large-scale financial loss.

ABOUT THE AUTHORS

Steve Tung (chstung@uark.edu) is an associate professor of mechanical engineering at the University of Arkansas, Fayetteville.

Michael B. Schulte (mshult@uark.edu) is pursuing his master's degree in mechanical engineering at the University of Arkansas, Fayetteville.

Zhuxin Dong (dzhuxin@uark.edu) is a Ph.D. student of mechanical engineering at the University of Arkansas, Fayetteville.

Jin-Woo Kim (jwkim@uark.edu) is an associate professor of biological and agricultural engineering at the University of Arkansas, Fayetteville.

Uche Wejinya (uwejinya@uark.edu) is an assistant professor of mechanical engineering at the University of Arkansas, Fayetteville.

Hyung-Mo Moon (hmoon@uark.edu) is a postdoctoral fellow of biological and agricultural engineering at the University of Arkansas, Fayetteville.

Byung-Whi Kong (bkong@uark.edu) is an assistant professor of poultry science at the University of Arkansas, Fayetteville.

REFERENCES

[1] E. Nester, D. Anderson, Jr., C. E. Roberts, and M. Nester, *Microbiology, A Human Perspective*, 5th ed. New York: McGraw Hill, 2007.

[2] H. Rokadia, B. Srinivasan, R. Wang, S. Tung, and Y. Li, "Characterization of avian influenza virus subtypes using atomic force microscopy," in *Proc. 9th IEEE Conf. Nanotechnology (IEEE-NANO)*, 2009, pp. 164–165.

[3] R. I. MacCuspie, N. Nuraje, S.-Y. Lee, A. Runge, and H. Matsui, "Comparison of electrical properties of viruses studied by AC capacitance scanning probe microscopy," *J. Am. Chem. Soc.*, vol. 130, no. 3, pp. 887–891, 2008.

[4] S.-W. Lee, Y.-W. Kim, and Y.-K. Kim, "Determination of dielectric constant of dielectric particles using negative dielectrophoresis," in *Proc. IEEE Annu. Report of the Conf. on Electrical Insulation and Dielectric Phenomena*, 1996, vol. 1, pp. 241–244.

[5] J. D. Jackson, *Classical Electrodynamics*, 3rd ed. New York: Wiley, 1998.